ELSEVIER
Materials Science and Engineering A299 (2001) 152–156
MATERIALS SCIENCE & ENGINEERING A
www.elsevier.com/locate/msea

Thermal fatigue of single-crystalline superalloy CMSX-4®: a comparison of epitaxial laser-deposited material with the base single crystal

L. Felberbaum [a], K. Voisey [a,1], M. Gäumann [b,2], B. Viguier [a,3], A. Mortensen [a,*]

[a] *Laboratoire de Métallurgie Mécanique, Department of Materials, Swiss Federal Institute of Technology in Lausanne (EPFL), MX-D Ecublens, CH-1015 Lausanne, Switzerland*

[b] *Laboratoire de Métallurgie Physique, Department of Materials, Swiss Federal Institute of Technology in Lausanne (EPFL), CH-1015 Lausanne, Switzerland*

Received 4 May 2000; received in revised form 28 July 2000

Abstract

The thermal fatigue resistance of cast single-crystalline CMSX-4 samples featuring an edge composed of a 1-mm-deep layer of laser-deposited epitaxial single-crystalline CMSX-4 is compared with that of samples made entirely of the virgin base material. Tests are conducted by cycling between 200 and 1100°C, and recording the progression of the largest crack growing in each sample. It is found that crack growth rates in samples with laser claddings are around twice those in the base material; this is chiefly attributed to their different thermal history. Resistance to crack initiation was lower in two out of three laser-clad samples than in the base material; this is attributed to interdendritic flaws in laser-clad layers of these two samples. The performance of the third coated sample was comparable with that of the base material.

Keywords: Thermal fatigue; Crack; Superalloy; Single crystal; Repair; Epitaxial laser metal forming

1. Introduction

Thermal fatigue (TF), caused by internal stresses generated by cyclic temperature gradients, is an important life-limiting factor for many operating parts at high-temperature such as turbine blades and vanes. Repair methods that extend the service life of components subjected to thermal fatigue are, thus, very attractive.

Epitaxial laser metal forming (E-LMF) may provide such a repair method. In this process, successive layers of material are deposited in the liquid state, and solidified in the presence of temperature gradients sufficiently steep to prevent, for the process conditions at hand, nucleation of the solid elsewhere than along the interface with the underlying base material [1]. The cladded solid therefore reproduces, by epitaxial growth, the grain structure of the substrate onto which it is grown. As a consequence, epitaxial laser forming can be used to repair a damaged single-crystalline superalloy component without introducing undesirable grain boundaries.

We report in what follows results from a study of the thermal fatigue performance of CMSX-4 single-crystalline superalloy samples 'repaired' by this technique, in which we compare the initiation and propagation of thermal fatigue cracks in the base material with that in an epitaxial laser cladding.

* Corresponding author. Tel.: +41-21-6932915; fax: +41-21-6934664.
E-mail address: andreas.mortensen@epfl.ch (A. Mortensen).
[1] Present address: Department of Materials Science and Metallurgy, Pembroke Street, University of Cambridge, Cambridge CB2 3QZ, UK.
[2] Present address: Calcom SA, CH-1015 Lausanne, Switzerland.
[3] Present address: Centre Interuniversitaire de Recherche et d'Ingéniérie en Matériaux (CIRIMAT), CNRS-ENSCT-INP, F-31077 Toulouse Cedex 4, France.

0921-5093/01/$ - see front matter
PII: S0921-5093(00)01378-2

2. Experimental procedures

The base material used in this study is CMSX-4® (Registered trademark of Cannon-Musgekon Corp.), a nickel-based single-crystalline superalloy (supplied by ABB Alstom Technology Ltd., Baden-Dättwil, Switzerland). Table 1 shows the nominal composition of this alloy [2].

The laser-clad material was grown epitaxially onto a cast single-crystalline substrate by the epitaxial laser forming process described in [1]. Process parameters are tailored according to solidification theory to grow sequentially epitaxial layers of superalloy material onto a CMSX-4 substrate. The powder used in the laser cladding process was of the same CMSX-4 composition given in Table 1.

Standard solutionizing and aging heat treatment procedures were applied by ABB to the base CMSX-4 single-crystalline material. After processing the laser-clad substrate was given an aging heat treatment only, because the laser-clad material was found to recrystallize when subjected to solution heat treatment temperatures [1]. The resulting microstructure of the laser-clad material is, hence, both finer (because of the far higher solidification rates) and chemically less homogeneous compared with that of the substrate CMSX-4 material (because of the absence of solution heat treatment).

The primary dendrite arm spacing was measured to be 10 μm in the laser cladding and 350 μm in the base material. Internal flaws of these materials were characterized using standard optical and scanning electron microscopy procedures. In the single-crystal CMSX-4 base material, internal defects took the form of rounded interdendritic micropores with a mean diameter of 15 μm. In the laser-clad material, internal defects were also interdendritic, taking three forms, (i) micropores about 10 μm in diameter on average; (ii) elongated interdendritic microcracks about 2 μm wide and resembling hot-tears; (iii) small islands of entrapped oxide, frequently associated with some microporosity.

Samples used for thermal fatigue testing had the dimensions and shape depicted in Fig. 1. These were electro-discharge machined from the ingot of base material, and then polished with diamond paste down to 1 μm. Care was taken to ensure that the ⟨001⟩ crystallographic 'low modulus' direction was parallel to the leading edge of the sample, as depicted on Fig. 1. This geometry, used in earlier work in our laboratory [3–6] can be regarded as a simplified version of the shape of the leading edge of a turbine blade, one TF-cycle simulating the start up and shutdown of the engine.

Table 1
Nominal composition of CMSX-4 (wt.%)

Cr	Co	Mo	W	Ta	Re	Al	Ti	Hf	Ni
6.5	9	0.6	6	6.5	3	5.6	1.0	0.1	Balance

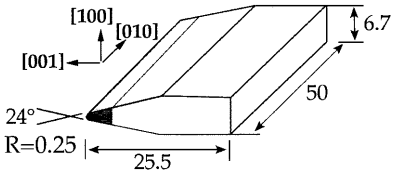

Fig. 1. Thermal fatigue specimen geometry and dimensions.

Laser-clad samples were similar in shape, the laser cladding forming the sample leading edge (as would be the case in a repaired turbine blade). These were produced by cladding a pre-machined parallelepiped 60 × 23.7 × 6.7 mm in size aligned along the ⟨100⟩ directions of the base single-crystalline material with a centrally located ridge of epitaxial laser-clad CMSX-4 material about 2-mm wide (Fig. 2). Clad samples were then machined to final shape and dimensions, and polished analogously to the base material samples. The resulting laser-clad section of the sample along its tip was about 1-mm deep after machining, and corresponded to the shaded area in Figs. 1 and 2.

The thermal fatigue test consists of repeated cycles of localized induction heating of the leading edge of the sample to 1100°C during 60 s, followed by cooling during 20 s to 200°C using a blast of air directed towards the leading edge. Type K thermocouples, spot-welded near the wedge tip, are used to monitor the temperature. The cycling is interrupted periodically for crack length measurement and sample inspection by scanning electron and optical microscopy. Data are plotted in the form of the length of the longest crack detected, a, measured perpendicularly to the edge on the side where the crack appears longest, as a function of the number of cycles, N. The thermal fatigue crack initiation and failure lives are, as in earlier work [5], defined as the number of cycles N_i and N_f corresponding to crack lengths of 0.1 and 1 mm, respectively. A detailed description of the testing procedure can be found in [3].

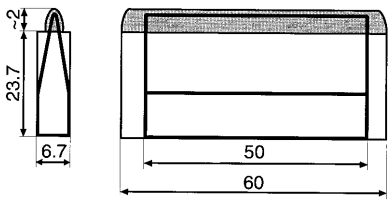

Fig. 2. Drawing of the laser-clad sample, epitaxial laser deposited material is in gray, and contours of the TF sample after machining are in bold.

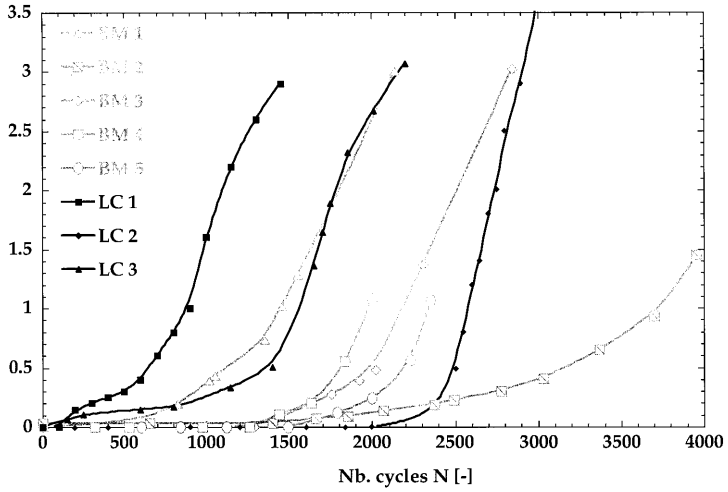

Fig. 3. Plot of longest fatigue crack length a as a function of number of thermal cycles, N.

3. Results

Eight samples were tested, three of which comprised an epitaxial laser-clad CMSX-4 layer along their leading edge. Several cracks were observed to initiate and grow during the test in all samples. As described above, the length of the longest crack is plotted in Fig. 3; this longest crack remained the same in all samples during the test (i.e. no crack overtook the longest crack). All crack length measurements were done on the side where the initiation occurred, the crack remaining longest on that side throughout the test.

Table 2 presents, in addition to N_i and N_f, four other parameters measured during the test; N_{both}, the number of cycles after which the crack starts to propagate on both sides of the sample, and a_{both}, the crack length at that time, Δ_{init}, the distance between the initiation site and the edge of the sample, and Δ_{I-II}, the crack length at the moment of change in propagation mode (detailed below).

In all five CMSX-4 base material samples, crack initiation occurred at pores located in the vicinity of the leading edge, at the surface of the sample or just below. In the laser-clad samples, crack nucleation consistently seemed to occur in solute-rich interdendritic areas of the microstructure. Often (but not always, since continuation of the test prohibited detailed metallographic examination of the growing cracks), the nucleation site of the cracks could be associated with identifiable processing flaws described above — pores, hot tears, or embedded oxides. This was true both for the largest cracks and also shorter cracks formed in the samples during the test.

In all samples crack propagation proceeded in inverse order compared with conventional fatigue testing of unnotched specimens; initially, the crack grew perpendicularly to the principal tensile stress axis, in mode II according to the conventional terminology. After growing to a certain length and traversing the specimen across its thickness, the crack propagation mode changed to mode I, namely shear along a $\langle 111 \rangle$ crystallographic plane as shown for a laser-clad sample in Fig. 4 (see also Table 2). In this second stage of crack growth, propagation was at a more or less constant rate, with relatively frequent crack branching occurring along other $\langle 111 \rangle$ slip planes.

Comparing the thermal fatigue crack nucleation and growth kinetics in the base and clad materials, Fig. 3, it is seen that,

1. in both data sets, there is considerable scatter in the overall fatigue life;
2. samples fail (i.e. the crack length a reaches 1 mm) relatively shortly after the onset of crack propagation on both sides of the specimen (this can be seen in Table 2. ($N_f - N_{both}$) is near 350 cycles for all specimens);
3. the rate of crack growth from N_{both} on is about twice as high in the laser-clad samples than in base material samples (between 3 and 6 μm per cycle vs. 1.5 and 3 μm per cycle, respectively);
4. the performance variation from sample-to-sample exceeds that between the average performance of the base material samples and that of the laser-clad samples.

4. Discussion

Results obtained on the base CMSX-4 material samples are in overall accordance with the data generated by Blümm on CMSX-4 using identical test conditions [4]. As in the present study, crack nucleation occurred at surface pores, which act as strain concentration sites and also as regions of preferential oxidation with con-

Table 2
Parameters measured during the test

Sample	Δ_{I-II} [μm]	Δ_{init} [μm]	a_{both} [μm]	N_{both} [−]	N_i [−]	N_f [−]	$N_f - N_{both}$ [−]
BM 1	650	350	530	1150	650	1450	300
BM 2	820	425	790	3525	1875	3715	180
BM 3	320	30	240	1635	1470	2185	550
BM 4	160	10	60	1345	1430	1975	630
BM 5	175	10	60	1660	1750	2335	675
LC 1	870	400	855	820	170	900	80
LC 2	500	100	160	2350	2300	2580	230
LC 3	1025	475	760	1485	225	1560	175

comittant formation of neighboring weaker γ′-denuded zones. The observed crack shapes, including the transition from mode II to mode I growth, are also comparable with what was found by Blümm. This transition can be ascribed to three factors, (i) stress gradients cause the crack tip stress intensity factor amplitude to decrease as the crack advances; (ii) the decreasing temperature at the advancing crack tip may also cause a transition in propagation mode (for example, Gabb observed that, under isothermal low cycle fatigue, the crack propagation mode changes from mode II to mode I all else being constant if the temperature is lowered from 980 to 760°C [7]); and perhaps also (iii) the change in crack shape, from semi-elliptical to roughly straight, once the crack has traversed the specimen width and propagates on both sides.

Comparing the two materials, one notes first the relative similarity in data between the virgin and laser-clad material. This result is a priori not expected given the significantly different microstructures of the two materials; the laser cladding features more microsegregation, a far finer microstructure, and a higher density of finer flaws (pores, microcracks, oxides) than the base material.

Crack propagation appears roughly similar between the laser-clad and the base material, save perhaps for a somewhat higher tendency in the laser cladding for crack branching and deviation to other ⟨111⟩ slip planes of similar Schmid factor during mode I propagation (Fig. 4). To compare crack growth rates in both sample types, we have replotted a versus N curves after shifting the origin of the crack cycle axis to the cycle at which the crack appears on both sides of the sample (i.e. the origin is shifted to N_{both} of Table 2, Fig. 5). It is seen that, although the curves superimpose relatively well, the crack growth rates in the repaired specimens are somewhat higher, by a factor near two as indicated above. One must note, however, that since the laser cladding is 1-mm deep, this slight difference in crack growth rates is not an inherent characteristic of the laser cladding, but of the repaired samples as a whole. The most likely explanation for the somewhat higher growth rates in clad samples therefore seems to be the difference in heat treatment between these and base material samples; the latter were submitted to full solution and aging heat treatment, whereas laser-clad samples were only aged after processing.

It is also clear from Fig. 5 that the significant scatter in fatigue life noted with both laser-clad and base material samples, Fig. 3, is linked with scatter in crack nucleation. The comparatively short initiation lives noted with two out of three laser-clad samples denote a

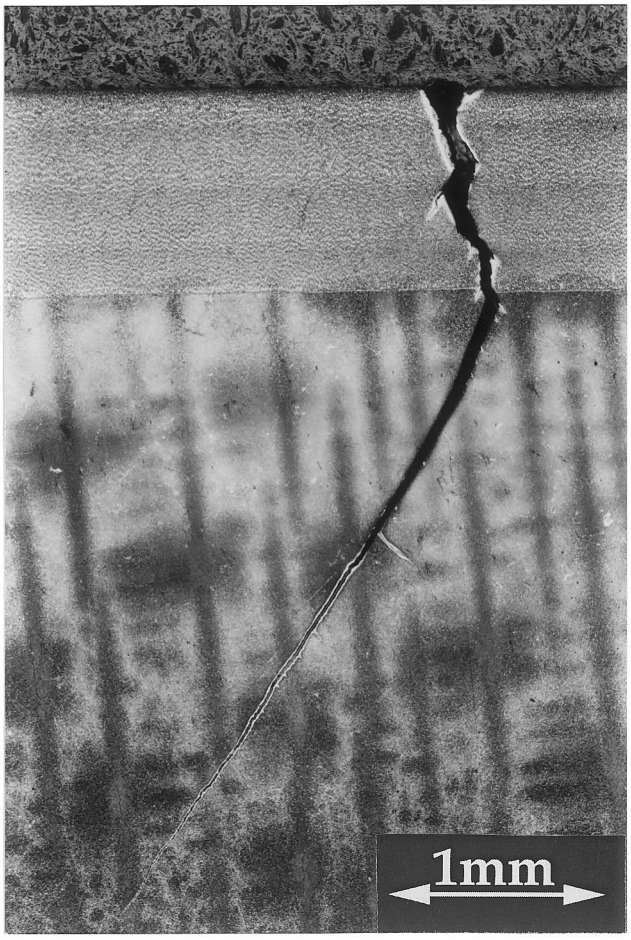

Fig. 4. Cross-section of thermal fatigue crack through a laser-clad sample (laser processed material on top, single crystalline substrate on the lower part of the picture).

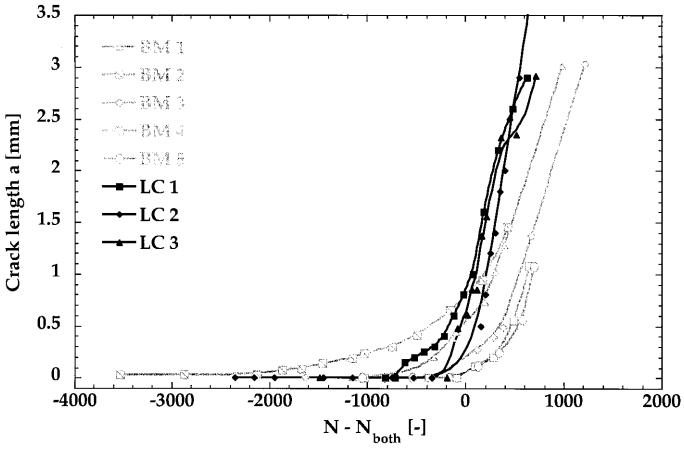

Fig. 5. Fig. 3 replotted after shifting the origin of the crack cycle N-axis to the cycle at which the crack appears on both sides of the sample (i.e. the horizontal axis is now ($N - N_{\text{both}}$, Table 2).

difference in the population of crack-nucleating flaws between the laser cladding and the base materials. Looking at the specific crack-nucleating defects in these three samples, we note that while in sample LC 2 (Table 2), no harmful defect was detected before cycling, interdendritic microcracks could be identified in sample LC 1. Similarly, the crack started in an interdendritic area in sample LC 3; however, no clear interdendritic defect was detectable before testing this sample. Initiation in sample LC 2 occurred at an internal pore, indicating that this specimen was free of microcracks, in any case in the vicinity of its leading edge. These microcracks, which resemble hot-tears in that they are interdendritic and perpendicular to the laser beam trajectory at the material surface, seem to be the most critical defects, worthwhile eliminating in optimization of the process. The fact that Sample LC 2 was seemingly devoid of such interdendritic cracks is encouraging in this regard.

5. Conclusion

We show that thermal fatigue performance is relatively similar in cast single-crystal CMSX-4 and in laser-deposited epitaxial single-crystal CMSX-4 layers for cycles between 1100 and 200°C. Resistance to crack initiation however was lower in two out of three laser-clad samples in comparison to the base material, due to interdendritic flaws. This, in turn, has two implications.

If interdendritic flaws in the epitaxial laser cladding can be eliminated or, at least, detected, this technique is viable for the repair of structures which must resist thermal fatigue.

When the technique is used to heal a crack within a component which has undergone prior cycling and therefore must be expected to contain other flaws, the performance of the repair is likely to be quite acceptable even though some defects may be present in the cladding. This is because the similar thermal fatigue crack growth rates between the base and clad materials will place similar limitations on the life that can be expected to remain in the structure.

Acknowledgements

This work was performed within the frame of the Swiss Priority Program on Materials Research in collaboration with ABB Alstom Power, Calcom SA, SR Technics and Sulzer Innotec AG. The authors would like to acknowledge the contributions of Jean-François Despois, Christopher San Marchi and Cyrille Bezençon in the course of this work.

References

[1] M. Gäumann, S. Henry, F. Cléton, J.-D. Wagnière, W. Kurz, Mater. Sci. Eng. A271 (1999) 232–241.
[2] K. Harris, G.L. Erickson, S.L. Sikkenga, W.D. Brentnall, J.M. Aurrocoechea, K.G. Kubarych, in: S.D. Antolovich, R.W. Stusrud, R.A. MacKay, D.L. Anton, T. Khan, R.D. Kissinger, D.L. Klarstrom (Eds.), Superalloys, Seven Springs Mountain Resort, Champion, PA, USA, The Metallurgical Society of AIME Publishers, Warrendale, PA, 1992, pp. 297–306.
[3] F. Meyer-Olbersleben, Thermische Ermüdung Einkristalliner Nickelbasis-Legierungen, Ph.D. thesis # 1255, Ecole Polytechnique Fédérale de Lausanne, Switzerland, 1994.
[4] M.R. Blümm, Einfluss der Anisotropie auf das thermische Ermüdungsverhalten von Nickelbasis-Legierungen, Ph.D. thesis # 1460, Ecole Polytechnique Fédérale de Lausanne, Switzerland, 1995.
[5] F. Meyer-Olbersleben, C.C. Engler-Pinto, F. Rézaï-Aria, in: M.J. Verrilli, M.G. Castelli (Eds.), Thermomechanical Fatigue Behavior of Materials, vol. 2, ASTM STP 1263, Philadelphia, PA, USA, 1992, pp. 41–55.
[6] F. Meyer-Olbersleben, D. Goldschmidt, F. Rézaï-Aria, in: S.D. Antolovich, R.W. Stusrud, R.A. MacKay, D.L. Anton, T. Khan, R.D. Kissinger, D.L. Klarstrom (Eds.), Superalloys, Seven Springs Mountain Resort, Champion, PA, USA, The Metallurgical Society of AIME Publishers, Warrendale, PA, 1992, pp. 785–794.
[7] T.P. Gabb, J. Gayda, R.V. Miner, Metall. Trans. A 17A (1986) 497–505.